A better understanding of orthodontic bracket bonding

Algera, T.J.

Publication date
2009
Document Version
Final published version

CHAPTER 7

A comparison of FEM-analysis with in vitro bond strength tests of the bracket-cement-enamel system

Submitted

7.1 Abstract

The aim of this study is to determine the *in vitro* shear and tensile bond strength of the bracket-cement-enamel system.

The shear strength was determined by loading the short and the long side of the bracketbase. Testing took place after storing the specimens 72 hours in 37ºC water. Fractures were analyzed with the adhesive remnant index (ARI) and scanning electronic microscopy (SEM). The stresses in the system were analyzed with finite element analysis (FEA) models of the experimental setup to identify the initial fracture point and the stress distribution at fracture. Statistical analysis was performed using ANOVA and the Tukey *post hoc* test for the bond strengths ($p < 0.05$).

The ARI scores were analyzed using the Kruskal-Wallis one way analysis of variance on ranks (ANOVA). ANOVA showed significant differences between the three experiments. Loading the short side of the bracket resulted in the highest average bond strength value. Tensile loading gave the lowest results. The finite element models (FEMs) were supported by the earlier bond strength findings and the SEM pictures. The finite element analysis (FEA) revealed peak stresses in the cement during loading and made clear that shear testing is sensitive to loading angles.

It is concluded that the stress distribution over the bracket-cement-enamel system is not homogeneous during loading. Fractures are initiated at peak stress locations. As a consequence the size of the bonding area is less predictive for bond strength values. The bracket design and the way of loading may be of more relevance.

7.2 Introduction

Bracket bond failure during an orthodontic treatment is a recurring event with the consequence that the bracket must be rebonded. This influences the treatment time negatively. The bracket failures are mostly explained by interfering with contact loading, improper performance of the bonding procedure, fatigue of the bonding material, or a combination of these factors.(1) To get an insight into the strength of the bracket-cement-enamel bond, *in vitro* tests are performed. With these tests the force necessary to debond a bracket is measured. The values are measured as force (Newton) but most often reported as strength (Pascal), which is calculated by dividing the force by the bonding area. Furthermore, the enamel specimen is usually examined under a microscope to identify the mode of failure; cohesive or adhesive. This mode of failure, which is represented in the adhesive remnant index (ARI), should give an idea of the weakest part of the bonding system.(2)

The variance among the reported bond strength values in different studies is probably caused by the amount of variables that is involved in these tests. This makes interpretation and comparison with existing literature data difficult. As mentioned above, the bond strength is reported in Pascal, which assumes that the complete bonding area is equally loaded at the measured force at fracture. According to finite element analysis (FEA) this is unlikely.(3) Katona showed that the force distribution during a shear, tensile or rotational test is not homogeneous at all.(3) It is most likely that a fracture, during loading, starts at a weak point in the system, usually a void, crack or at the border of the bracket.(4) Because of the brittle nature of the cement (4) these initial cracks lead to complete fracture and debonding of the bracket. The elastic property of the bracket and the cement used, play a role in the debonding, which is confirmed by the difference in bond strength between ceramic and stainless steel brackets bonded with the same cement.(5) It is therefore interesting to get an insight in the stress distribution prior to debonding and the location of the fracture initiation. Together with knowledge of the fracture propagation pattern and the force measured at debonding this can lead to a better understanding of bracket bond failures and eventually to prevention of this problem.

The aim of this study is to reveal the fracture mechanisms of bracket debonding by applying finite elemental analysis (FEA) on *in vitro* bond strength test specimens and scanning electronic microscopic (SEM) photographs.

7.3 Materials and methods

In this study the tensile and shear bond strength of the bracket-cement-enamel system were measured and their fractures were analyzed using Scanning Electronic Microscopy (SEM). The obtained tensile and shear bond strength were used as input for finite element modelling and analysis of the test specimen.

Specimen preparation

Enamel specimens were made of bovine teeth, collected from 2 year old cattle. The crowns of the teeth were sectioned from the roots and embedded in Polymethyl methacrylate (PMMA). After setting of the PMMA, the buccal surfaces were ground with sandpaper until grit 1200, ensuring a standard smooth bonding surface. Mesh based brackets (Mini Twin, "A"Company Orthodontics, San Diego, CA, USA; size 3.0 x 4.2 mm), intended for bonding to central upper incisors, were bonded to these surfaces using Transbond XT (3M Unitek, Monrovia, Ca, USA). Pre-treatment of the bonding area was according to the manufacturers instructions and consists of 35% phosphoric acid etching (Ultradent Products, South Jordan, Utah, USA) followed by the application of a thin layer of adhesive resin (3M Unitek, Monrovia, California, USA). Light curing was performed using a Elipar Trilight curing unit (3M-ESPE Dental Products, Seefeld, Germany) in a standard mode at 750 mW/cm^2. Fifteen specimens per group were stored in tap water of 37°C for 72 hours.

Tensile and shear bond strength determination

The tensile bond strength was determined as previously described.(6) The specimens were attached to the crosshead using a round stainless steel wire with a diameter of 1 mm bend in a U-form and tied with a harness ligature to the bracket. The free ends of the wire were clamped in the connecting piece of the crosshead. A hinge in the connecting piece together with the round wire made vertical alignment of the specimen possible (vertical alignment is necessary for homogeneous stress distribution during the test). The shear bond strength was determined in two directions. The brackets were loaded at the short and the long side of the bracket. For both tests the specimens were placed in a brass block in which the bracket was located exactly at the edge of the holder as described previously (Chapter 6). The bond strength tests were carried out in a universal testing machine (Hounsfield Ltd., Redhill, Surrey, UK) at a crosshead speed of 0.5 mm/min. Average tensile and shear bond strengths were calculated by dividing the measured load at fracture by the bonding area.

After testing, the type of fracture was scored using the adhesive remnant index (ARI) (2) to identify the weakest point in the bracket-cement-enamel system. A score of 0 indicates that no adhesive was left on the enamel, 1 indicates that less than half of the adhesive remained, 2 indicates more than half of it remained, and 3 indicates that all the adhesive remained on the enamel surface. The scores were determined with a stereomicroscope at a magnification of 25x.

Statistical analysis

One-way analysis of variance (ANOVA) was used to test the effect of the different test methods. The Tukey *post hoc* test was performed to show individual differences. Differences in ARI scores were analyzed using the Kruskal-Wallis one way analysis of variance on ranks. A P-level <0.05 was considered significant. The software used was SigmaStat Version 3.0 (SPSS Inc, Chicago, USA).

SEM analysis of the specimens

After fracture, one specimen of each test mode was selected for SEM analysis of the fracture surface. These specimens were gold plated using a sputter coater (Edwards Sputter Coater S 150B, Edwards and Philips, West Sussex, England). Examining took place with a Scanning Electronic Microscope (20 XL, Philips, Eindhoven, The Netherlands) at a 25x magnification.

Finite element analysis

A three-dimensional simplified finite element analysis (FEA) model with the three loading modes of the bracket-cement-enamel system was created. The finite element modelling was carried out with FEMAP software (FEMAP 8.10, ESP, Maryland Height, MO, USA), while the analysis was carried out with CAEFEM 7.3 (CAC, West Hills, CA, USA). The dimensions of the enamel block representing an abutment tooth, were 6.0 mm long, 5.0 mm width, and 1.0 mm in height. The cement layer was 4.2mm long, 3.0 mm width and 200 μm in height. The dimensions of the bracket-cement-enamel system are represented in Figure 7.1. The models were composed of 23,392 parabolic hexagonal solid elements. The material properties (Table 7.1) were assumed to be isotropic homogenous and linear-elastic.(7, 8) The nodes at the bottom of the enamel were fixed (no translation or rotation in any direction). To make the results comparable, a standardized load of 100 N was applied at the points indicated with arrows in Figure 7.2. With the peak stress results of the

virtually loaded models and the obtained average bond strength results of the *in vitro* tests, the peak stresses inside the specimens at fracture could be calculated.

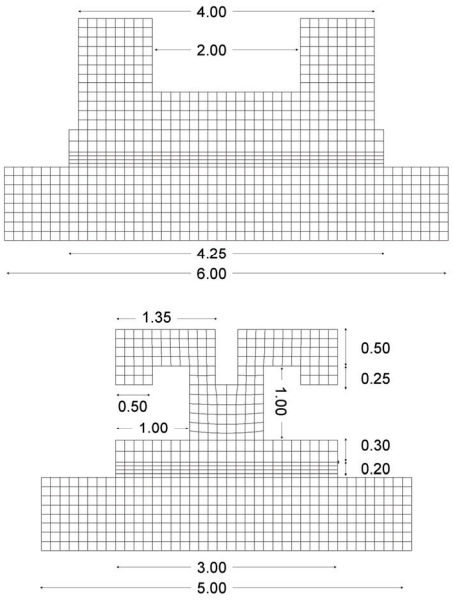

Figure 7.1 The geometric measures of the bracket-cement-enamel system. The upper drawing shows an occlusal view. The lower drawing is viewed from a mesial or distal side.

Table 7.1 The elastic properties of the materials used in the finite element model.

Material	Young's modulus (MPa)
Stainless steel	210,000
Enamel	84,000
Composite (Transbond XT)	5,000

7.4 Results

The results of the three bond strength tests are summarized in Table 7.2. The lowest bond strength values are observed with the tensile test, while the shear tests resulted in significant higher bond strength values. Comparing the shear tests shows that loading the short side gives higher fracture bond strength values compared to loading the long side. The ARI scores (see Table 7.3) of the three test modes did not differ significantly. The average score was between 2 and 2.5 indicating that most of the adhesive remained on the enamel. After fracture the specimens are also studied with SEM. The specimens that are loaded on the long or short side show a fracture pattern which starts adhesively between the cement and the bracket and changes into a

cohesive fracture (see Figure 7.4A and 7.4B). The tensile loaded specimens show a completely adhesive fracture between the bracket and the cement (see Figure 7.4C).

Table 7.2 The average bond strengths in N and MPa together with the standard deviations. The small letters indicate a significant difference between the tests at a P-level of 0.05. In the third column the peak stresses are calculated on basis of the FEMs. The results of the shear tests are calculated with a loading angle of 0 degrees.

	Force (Newton)	Strength (MPa)	Calculated debonding peak force (Newton)
Tensile strength	69.4[a] (5.7)	5.7[a] (1.8)	17.9 (1.5)
Shear strength long side	117.4[b] (9.6)	9.6[b] (2.5)	18.7 (1.5)
Shear strength short side	153.9[c] (12.4)	12.4[c] (2.8)	31.1 (2.6)

Table 7.3 The ARI-scores and the average ARI score.

Test	0	1	2	3	Average
Shear long	1	3	4	7	2.3
Shear short	0	2	7	6	2.3
Tensile	0	2	6	7	2.1

The FEM represents a stainless steel bracket bonded to enamel with a composite cement. The models with the different loading modes; (A) tensile, (B) long side, and (C) short side, are shown in Figure 7.2. The sectional view of the cement layer depending on the three loading modes; (A) tensile, (B) long side, and (C) short side loading mode are shown in Figure 7.3. The obtained results show that the force distribution of the three different loading modes is not homogeneous. Tensile loading gives rise to the highest peak stress located at the short sides of the bracket (25.8 MPa), while loading the system on the long and short side results in 15.9 and 20.6 MPa, respectively. With these results the peak stresses responsible for the fracture of the *in vitro* specimens could be calculated. The values are presented in the third column of Table 7.2. Based on the experimental data it was expected that the peak stress of the short side loading situation would have been the lowest. For that reason the load angle on the model with load on the short side is varied between 0-10°. The calculations on the different loading angles result in different stress distribution and peak stresses. The results are graphically depicted in Figure 3D – H.

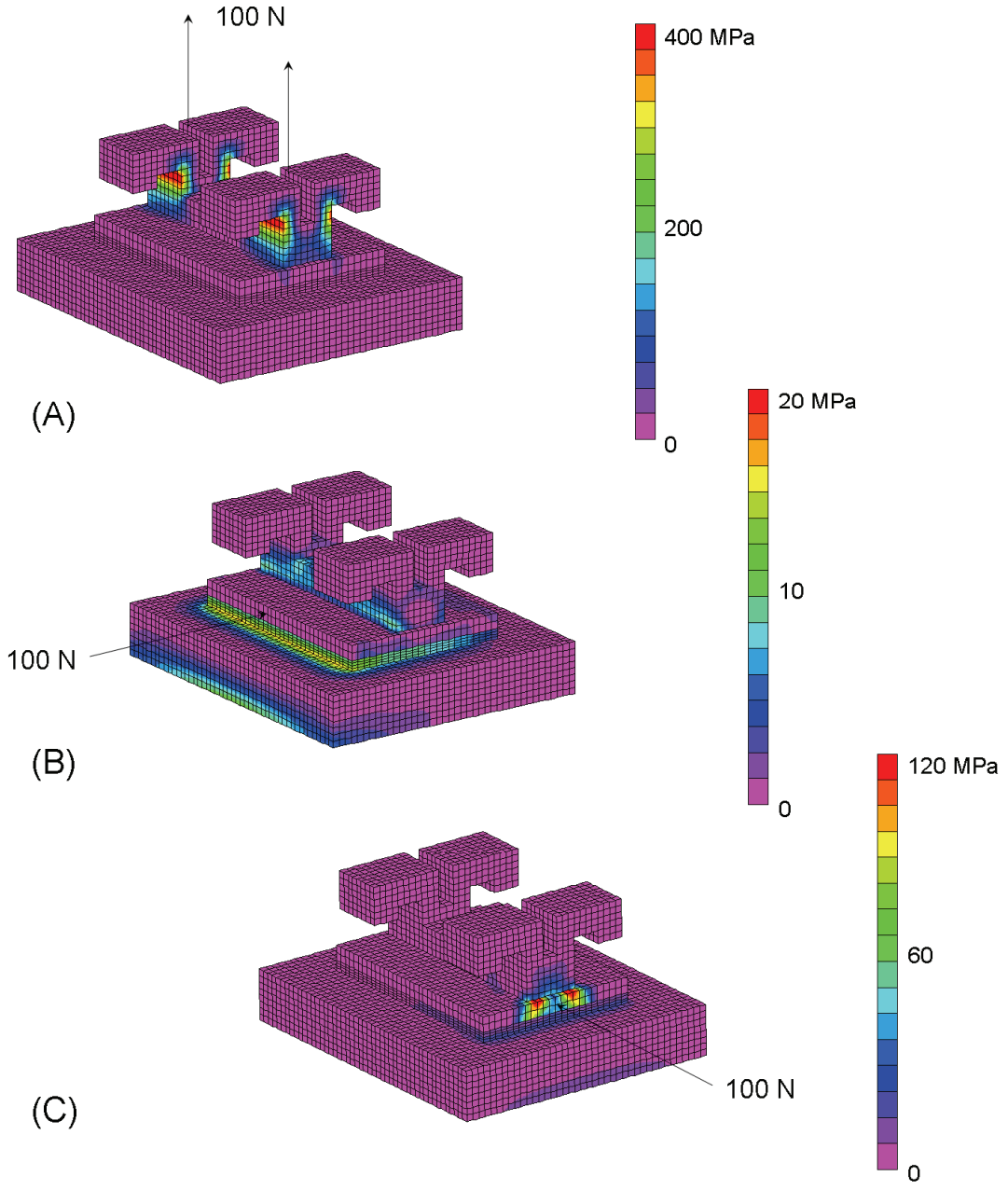

Figure 7.2 The FEMs of the bracket-cement-enamel system. The loading vector is indicated with an arrow. All models are loaded with 100 N. The colors show the resulting stress distributions during loading in MPa.

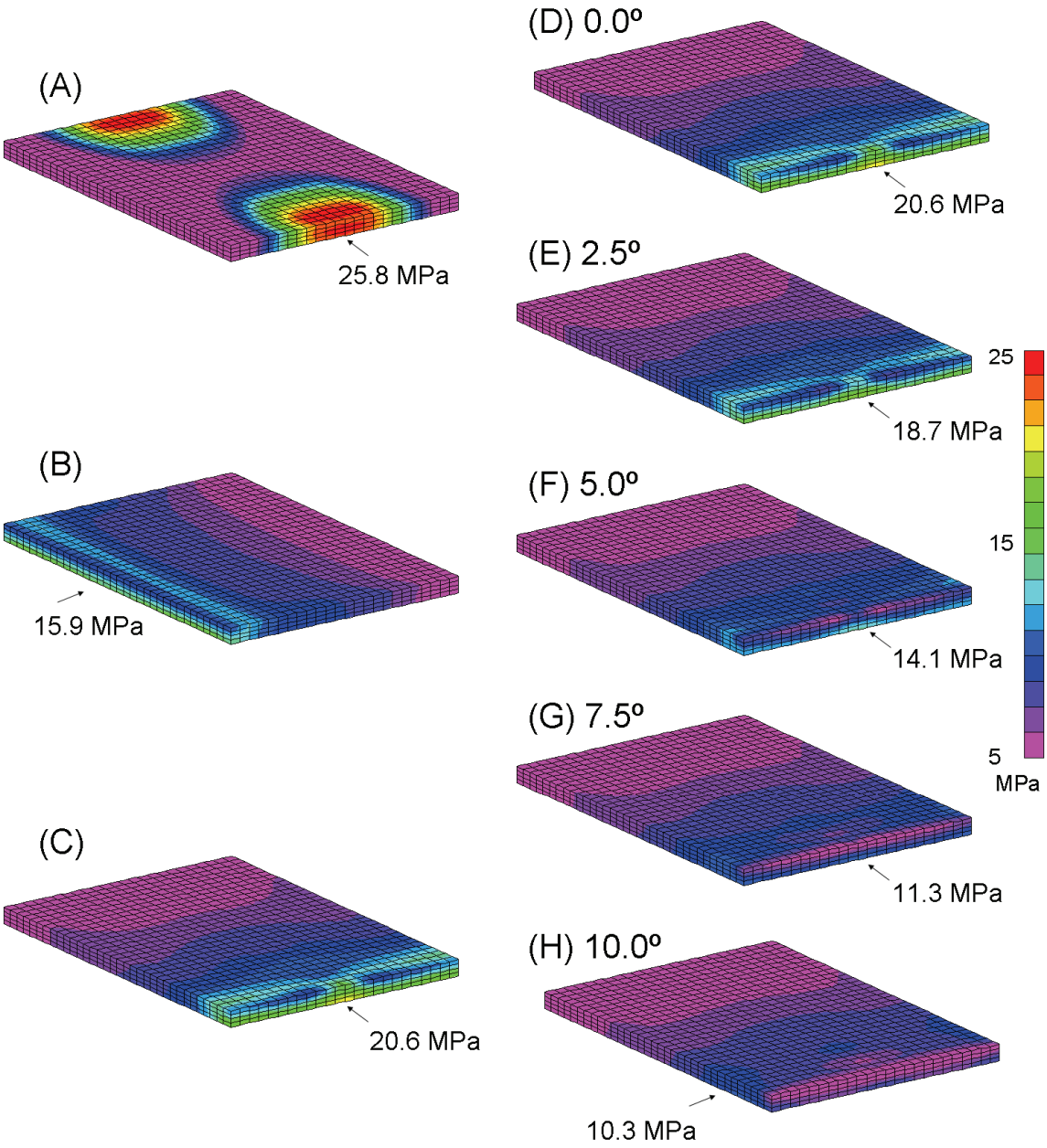

Figure 7.3 The stress distributions during loading in the cement layer. The colors represent the actual stress when the bracket is loaded with 100 N. The Figures A, B and, C show the cements of the three different loading procedures. At the right side (D, E, F, G and, H) shear loading of the short bracket side is shown under different angles.

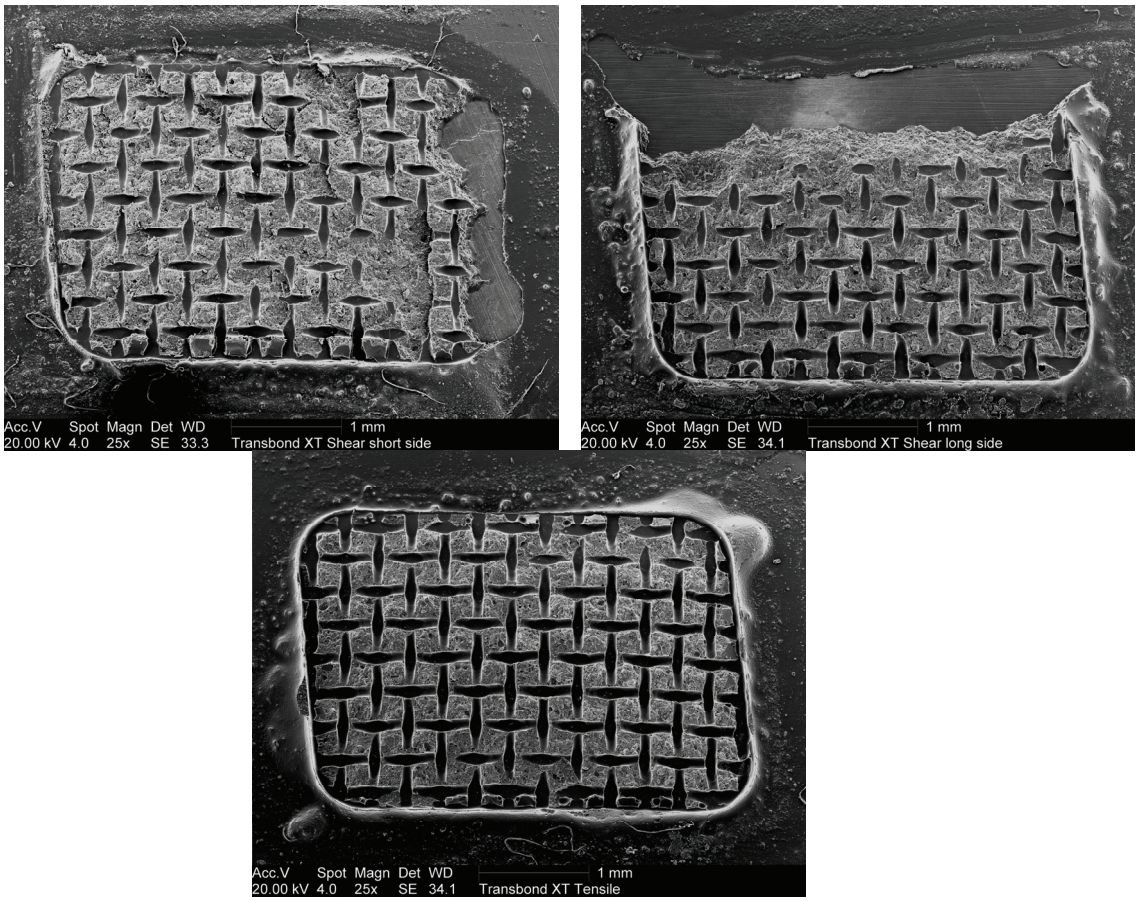

Figure 7.4 A, B and, C: The SEM pictures show the bonding areas of the debonded specimens. The upper two underwent a shear test. The left specimen is loaded at the short left side, the right one is loaded at the long side at the bottom. The lower picture is loaded in a tensile way. The fracture patterns resulting from both shear tests give a rather similar view. The fracture starts cohesively at the pressure side and transfers in an adhesive failure at the far end the bonding area. Difference between the two is the presence of fracture lines in the specimen loaded at the short side which run perpendicular at the loading direction. These lines are not present in the specimen loaded at the long side. The specimen loaded in a tensile way does not show a clear fracture pattern. The start of the crack at one of the short sides is most likely.

7.5 Discussion

The *in vitro* bond strength is tested in tensile and shear. The latter test was performed in two modes; the short and long side of the base, respectively. Significant differences in bond strength between tensile and shear tests are reported.(9) That

significant differences, measured between the two shear tests, can occur is in general not well recognized. The location of loading is usually not reported in the literature. The obtained results clearly demonstrate that the location of the load and the stress distribution inside the bracket-cement-enamel system is an important parameter in strength testing.

In a previous study specimens consisting of small stainless steel buttons with a round base bonded with Transbond XT to bovine enamel were investigated (Chapter 6). The shear bond strength for the bracket-cement-enamel system was found to be 23.7 MPa. This shear bond strength is higher compared to the shear bond strength values of this study (9.6 MPa and 12.4 MPa for loading the long and short side respectively). Apparently, small stainless steel buttons with a round base distribute the applied load better resulting in relative lower local peak stress and as a result a higher shear bond strength. That stress distribution play an important role in tensile and shear testing has already been recognized. For that reason tensile and shear testing is commonly performed on small specimens (< 1 mm^2), e.g. micro tensile and shear bond strength testing.

In order to understand the peak stress and distribution during load of the bracket-cement-enamel system a FEM was created. When a standardized load of 100 N was applied to the model a peak stress of 25.8 MPa within cement layer was found. Experimentally an average load of fracture of 69.4 N was observed. From these values one can estimate that the experimental peak stress within the cement layer causing the failure was 0.694 x 25.8 = 17.9 MPa. For the shear bond strength with loading on the long side an experimental peak stress of 18.7 MPa was found. These two values are in good agreement and close to the 23.7 MPa which was previously observed with the small round buttons. The shear bond strength with loading on the short side resulted in an experimental peak stress of 31.1 MPa, which is much higher compared to the two other values. A straightforward explanation based on stiffness, curvature of the bracket, cement layer thickness, could not clarify this observation completely. A close look at the design of the bracket revealed that the bracket base and the wings have exactly the same dimensions (see Figure 7.1). Therefore, if the edge of bracket base and wingtip are in contact with the base plate of the shear bond testing device the bracket base is always exactly parallel to the loading direction. The shear bond test which was loaded on the short side is in this respect different, *i.e.* the bracket base is larger than the wings. During the testing in the universal testing machine the specimen has some degree of freedom, which can result in a small angle between the bracket base and the loading direction. A small variation in loading angle may have a relative

high effect on the peak stress. This was investigated with a FEA (see Figure 7.3). The analysis showed that variation in the loading angle and bracket base between 0 and 10º resulted in a peak stress from 20.6 to 10.3 MPa, respectively. Based on the experimental determined shear bond strength is the angle in the experiments was approximately 7.5º.

The SEM pictures and de high ARI scores showed that the weakest point in the bracket-cement-enamel system is the cement bracket side. The fracture patterns of the tensile test showed a clear debonding between the cement and the bracket, while the shear test showed a more complex but reproducible fracture pattern. During loading the initial stress is localized in the cement on the edge of the bracket, as was shown by the FEA analysis. When the peak stress exceeds the bond strength between the cement and the bracket a crack develops, which travels at this interface. At a certain point the bracket starts to behave like a cantilever. At that moment the loading direction changes in a combined tensile-shear force resulting in a cohesive fracture pattern. After fracture most of the adhesive remained at the enamel side. An explanation for this finding is the presence of more defects at the bracket side compared to the enamel side. Fractures start at locations in the bonding area where these defects are present and the stress is high.(4)

7.6 Conclusions

Loading a bracket at the short side resulted in a significant higher bond strength compared to loading at the long side. This could be explained by the angle of loading. The highest stress concentrations during shear loading are located at the side of loading. The obtained results were rationalized with the FEA. The models showed a large stress non-homogeneity of the bracket-cement-enamel system during loading and the usefulness of these models was supported by the *in vitro* test results and the SEM photographs. Because of the difficulty of controlling the loading angle in most shear tests, bond strength testing for comparison and clinical reasons can be best performed in a tensile mode instead of a shear mode.

7.7 References

1. O'Brien KD, Read MJ, Sandison RJ, Roberts CT. A visible light-activated direct-bonding material: an in vivo comparative study. *Am J Orthod Dentofacial Orthop* 1989 **95**:348-51.
2. Artun J, Bergland S. Clinical trials with crystal growth conditioning as an alternative to acid-etch enamel pretreatment. *Am J Orthod* 1984 **85**:333-40.
3. Katona TR. A comparison of the stresses developed in tension, shear peel, and torsion strength testing of direct bonded orthodontic brackets. *Am J Orthod Dentofacial Orthop* 1997 **112**:244-51.
4. Higg WA, Lucksanasombool P, Higgs RJ, Swain MV. Evaluating acrylic and glass-ionomer cement strength using the biaxial flexure test. *Biomaterials* 2001 **22**:1583-90.
5. Haydar B, Sarikaya S, Cehreli ZC. Comparison of shear bond strength of three bonding agents with metal and ceramic brackets. *Angle Orthod* 1999 **69**:457-62.
6. Algera TJ, Kleverlaan CJ, de Gee AJ, Prahl-Andersen B, Feilzer AJ. The influence of accelerating the setting rate by ultrasound or heat on the bond strength of glass ionomers used as orthodontic bracket cements. *Eur J Orthod* 2005 **27**:472-6.
7. Geng JP, Tan KB, Liu GR. Application of finite element analysis in implant dentistry: a review of the literature. *J Prosthet Dent* 2001 **85**:585-98.
8. Walker MP, Spencer P, Eick JD. Effect of simulated resin-bonded fixed partial denture clinical conditions on resin cement mechanical properties. *J Oral Rehabil* 2003 **30**:837-46.
9. Katona TR, Long RW. Effect of loading mode on bond strength of orthodontic brackets bonded with 2 systems. *Am J Orthod Dentofacial Orthop* 2006 **129**:60-4.